Journal of Physics: Conference Series

Synthesis and characterization of ZnO nanoparticles using sol gel technique for dye sensitized solar cells applications

IOP Conf. Series: Journal of Physics: Conf. Series **1294** (2019) 022022 doi:10.1088/1742-6596/1294/2/022022

Synthesis and characterization of ZnO nanoparticles using sol gel technique for dye sensitized solar cells applications

H Musleh[1,2], H Zayed[2], SShaat[3], H MTamous4, J Asad1, A Al-Kahlout[1], A Issa[5], N Shurrab[4] and N AlDahoudi[1]

[1]Al Azhar University-Gaza, Physics Department, Gaza, Palestine, P.O. Box 1277
[2]Ain Shams University, Women`s College for Art, Science, and Education, Physics Department ,Cairo, Egypt
[3] Islamic University of Gaza, Physics Department, Gaza, Palestine, P.O. Box 108.
[4]Alzhar University-Gaza, Chemistry Department, Gaza, Palestine, P.O. Box 1277
[5]Azhar University-Gaza, Engineering Department, Gaza, Palestine, P.O. Box 1277

Email: h.mphysics@hotmail.com

Abstract. ZnO nanoparticles were synthesized using sol gel technique at different calcination temperature. The effect of calcination temperature on the structure and optical properties of ZnO NPs were studied in detail by using different techniques, X-ray diffraction, high-resolution transmission electron microscope, UV-VIS spectroscopy and photoluminescence spectroscopy. X-ray diffraction analysis revealed that the ZnO NPs were crystalized in a wurtzite structure and the estimated average particle size increased from 24.7 to 40.4 nm with increasing calcination temperature. In addition, the d spacing increased from 0.28196 nm to 0.28213 nm. High-resolution transmission electron microscopy analysis image showed spherical ZnO NPs were formed. UV-VIS absorption measurement was employed to evaluate the absorption edge and the optical band gap using Tauc plot. Energy gap revealed a red shift from 3.15 to 2.96 eV when the calcination temperature was increased. Dye sensitized solar cells were fabricated using synthesized ZnO NPs as a semiconducting layer that were dyed with different Xanthene (CH2[C6H4]2O) dyes separately; (Eosin B, Eosin Y and Rhodamine B) which are low cost dyes. Thin layer of ZnO were deposited on transparent fluorine doped tin oxide conductive glass using doctor blade method. Eosin Y exhibited the best photosensitizing. The conversion efficiency showed a significant improvement from 0.1% to 1.08%.

key words: ZnO NPs, Eosin Y, Eosin Y, Rhodamine B, Sol gel, energy gap, and Dye sensitized solar cells.

1. Introduction

Zinc oxide (ZnO) is a versatile material that has realizable applications in photocatalysts [1], piezoelectric[2], Transducers, varistors [3], solar cells[4], and transparent electrodes [5]. In addition, ZnO have a wide band gap about 3.37 eV and large excitation binding energy (60 meV) [6]. Which confirms a great effective of UV-blue emission in electrooptic devices, UV and high energy laser diodes at room temperature[7]. It have been integrated into many industrial branches such as health,

food, chemical, and cosmetics industry. Recently, a green and environment-friendly techniques have been used for ZnO NPs synthesis through bacteria, plants, algae, fungi [8]. There are numerous techniques that have been put forward for synthesis of these nanoparticle materials[9], namely, dip coating[10], refluxing and sol gel[11]. Sol-gel technique is a possible technique that, it is relatively low cost in process ZnO nanoparticles, simple and it does not need to be treated in relatively high growth temperature catalyst free growth, environmental friendliness, less hazardous and large area uniform production [12]. In this work, ZnO nanoparticles were synthesized by using sol-gel method, in an attempt to find the optimum conditions to produce ZnO nanoparticles with relatively small size at the low calcination temperature as well as to investigate the effect of calcination temperature in the structure and the optical characteristics of synthesized ZnO nanoparticles. In addition, the DSSCs were fabricated using ZnO nanoparticles as a semiconducting layer that were photosensitized with different three dyes. These dyes were characterized by UV-VIS spectrophotometry. The photovoltaic properties of the fabricated DSSCs were investigated as well.

2. Experimental

Zinc acetate dihydrate ($Zn(CH_3COO)_2.2H_2O$) salt ≥ 99.9% assay from Merck (ZA) and oxalic acid ($H_2C_2O_4.2H_2O$) ≥ 99.9% assay from Merck (OA) were used without further purification. ZA solutions were prepared by dissolving 2.7g of ZA into 35 ml of absolute methanol (CH_4O) ≥ 99 % assay from SDFCL (Me) under vigorous stirring for 30 min at 60 ^oC followed by sonication until clear and transparence solution were obtained (solution A). In the same way, 3.15 g of (OA) was dissolved into 10 ml of tribal distilled water at 60 ^oC and it was kept under constant stirring for 30 min to complete dissolving, followed by sonication (solution B). OA solution was added drop wise to the ZA solution under vigorous stirring. A white suspension was formed under a continuous stirring at 60 ^oC for 1hr. The suspension was left at 25 ^oC under slow stirring for 12 hr. The white suspension was washed by dispersion in absolute ethanol five times using centrifugation at 3500 rpm then dried at 90 ^oC for 12 hr. The powder was calcinated at different temperature 350 ^oC (O1), 400 ^oC (O2), 450 ^oC (O3) and 500 ^oC (O4) for 1 hr. Finally, the product was crashed gently using mortar and pestle to produce a fine powder. Flowchart for the preparation of ZnO NPs using sol gel technique is illustrated in Figure 1.

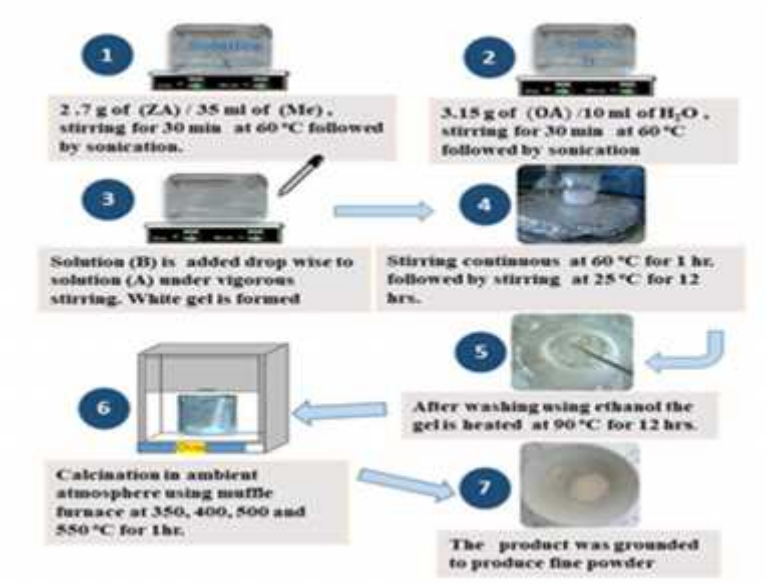

Figure 1. Flowchart for the preparation of ZnO NPs using sol gel technique.

Crystal structure identification and crystal size analysis were performed with X-ray diffractometer Philips Expert, with Cu-K_α radiation source (λ=1.5418 Å) and scan rate of $0.5^\circ min^{-1}$. High-resolution transmission electron microscopy analysis (HRTEM) was achieved with (JEM-2100), 200 kV. The images were taken after suspending the NPs in absolute ethanol. The UV-VIS absorption spectra were taken using double beam Shimadzu UV-1601 PC of ethanolic nanoparticle solutions made by sonication of the ZnO powder in absolute ethanol. The photoelectrochemical measurements of the DSSCs under illumination were performed using a personal computer controlled Elvis National Instruments in combination with a LabVIEW program. The illumination light intensity was about 100 $mWcm^{-2}$.

3. Ffabrication And Assembly Of The Dsscs Devices

Fluorine-doped SnO_2 (FTO with 10 Ωcm^{-2}, 80 % visible transmittance) coated glass substrates were used to build the DSSCs device. The FTO substrates. Cleaning process of FTO substrate and details of fabrication of the DSSCs devices was discussed elsewhere in our previous work [4]. The sensitized films were rinsed in ethanol and were dried in air at room temperature. A Pt-coated glass substrate was used as the counter electrode where the liquid electrolyte (a redox) (I^-/I^{-3}) electrolyte solution was composed of 0.334 g of LiI, and 0.0317 g of I2 dissolving in 4 mL of propylene carbonate and 1mL of acetonitrile.

4. Results And Discussion

4.1. X-Ray Diffraction Study

Figure 2 shows the X-ray diffraction (XRD) patterns of synthesized ZnO nanoparticles (ZnO NPs) samples at different calcination temperature (CT). The XRD analysis for the samples (O1, O2 and O3) exhibit a hexagonal wurtzite structure that are in good agreement with data reported in the literature (ICSD card number 067454). In addition, the experimental XRD results are in good agreement with the reported[13]. Furthermore, no detected peaks corresponding to any impurity could be noticed that confirms the formation of single phase of ZnO NPs. The preferred alignment corresponding to the Miller indices plane (101) is the most dominant peak, which overcomes the other peaks. These results are in agreement with the obtained results in[14]. At low CT (O1 sample), it is clear that, a presence of characteristics peaks of $Zn(OH)_2$, but by increasing the CT (O2, O3, and O4 samples) causes a transition from $Zn(OH)_2$ to ZnO [10]. Form Figure 2 the intensity and the sharpness of the XRD peaks increased with the increasing of the CT. This is an indicator to the increasing of the crystal size[15]. However, CT is a central factor to effect of the structural of ZnO NPs. [16]. In addition, the experimental values of lattice constant a = 0.325 nm and c = 0.522 nm, which corresponds to ZnO. The average particle size of the ZnO NPs were estimated from the broadening of the highest intensity peak (101) by Debye-Scherrer's equation[17]. The average size of the NPs increased from 24.7 to 40.45 nm with increasing CT. Geometric parameters for synthesized ZnO NPs at different CT are listed in Table I.

Table 1. Geometric parameters for O2, O3 and O4 of ZnO NPs.

#	**a (nm)**	**c (nm)**	**d (nm)**	**ca^{-1}**	**V_{UC} (nm^3)**	**D (nm)**
O2	0.32393	0.52027	0.281964	1.6061	0.047277	24.70
O3	0.32494	0.52038	0.282013	1.6015	0.047582	35.43
O4	0.32500	0.52100	0.282125	1.6031	0.047657	40.45

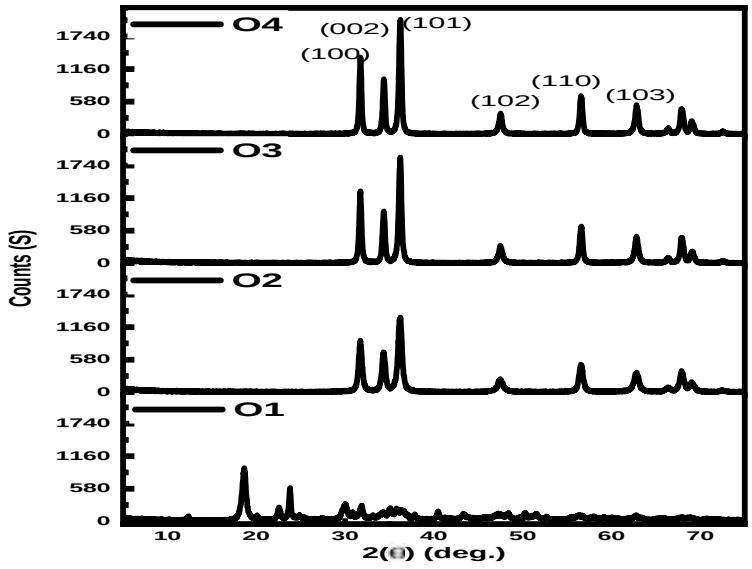

Figure2. XRD patterns of the synthesized ZnO NPs

4.2. Hrtem Analysis Of Zno Nps

The morphology of the ZnO NPs was investigated by high-resolution transmission electron microscopy (HRTEM). Figure 3(A) illustrates the micrograph image of O2 sample of ZnO NPs. As shown in this Figure, ZnO NPs have a good crystalline, with spherical and uniform shape. The inset in Figure 3(B) reveals that the interlayer spacing of 0.216 nm corresponding to the d-spacing of (101) planes (d101 = 0.221 nm from XRD calculation) in wurtzite ZnO. The size distribution of ZnO NPs are given by mean ± standard deviation (SD) that can be established from the fitting of the histogram by normal function (solid brown line in Figure 3 (B)). Furthermore, the estimated average size distribution of ZnO NPs is 27.01±2.66 nm. It is much closed to that estimated size from the XRD patterns using Scherrer's method (D =24.70 nm).

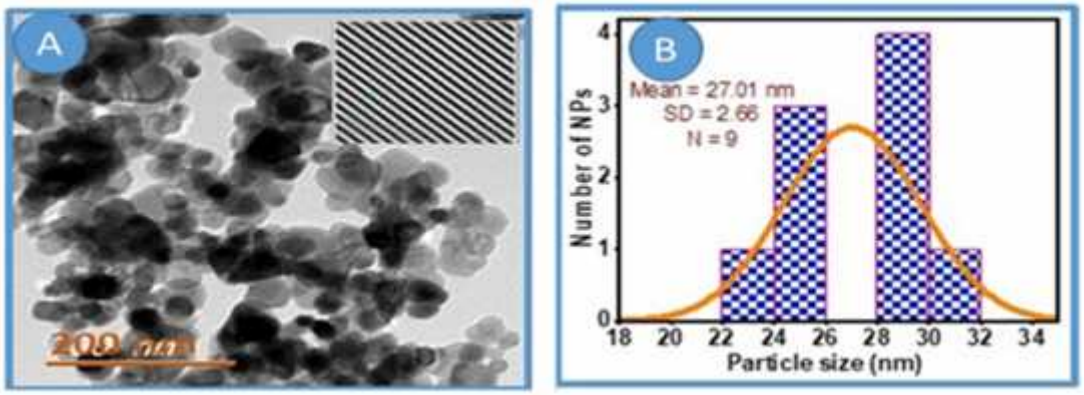

Figure 3. HRTEM image of O2 ZnO NPs,
(A) HRTEM micrograph image, (B) crystallite size histogram.

4.3. Uv-Vis Absorption Studies

The effect of CT on the optical properties of ZnO NPs was studied by UV-VIS absorption spectroscopy. The absorption as a function of the wavelength was measured over the range (300-800nm) at room temperature. Figure 4 depicts that the ZnO NPs has a very high absorbance in the UV region and then it decreases exponentially with increasing of the wavelength, which indicates that ZnO NPs have a high response in the UV region. This Figure indicates that, the corresponding absorption edge was 375.9 nm, 376.2 nm, and 377 nm where the CT about 400 ^{o}C, 450 ^{o}C, and 500 ^{o}C, respectively. The standard UV absorption peak of bulk ZnO about 388 nm[18]. It is clear that the absorption peak shifted to lower wavelength. This shift may be attributed to the quantum confinement effect [19]. Further, a noticeable a red shift in the absorption edges is observed with increasing of CT. This red shift indicates an increases in the particle size. The energy band gap (Eg) can be estimated from the absorbance spectrum was calculated using Tauc relation. Figure 5 indicates that the energy gap (Eg) decreases from 3.15 eV to 2.96 eV, where the CT increases from 400 ^{o}C to 550 ^{o}C. The variation of the Eg and D as a function of CT of ZnO NPs are summarized in Figure 5. Same result have been reported for ZnO NPs in many literatures[20].

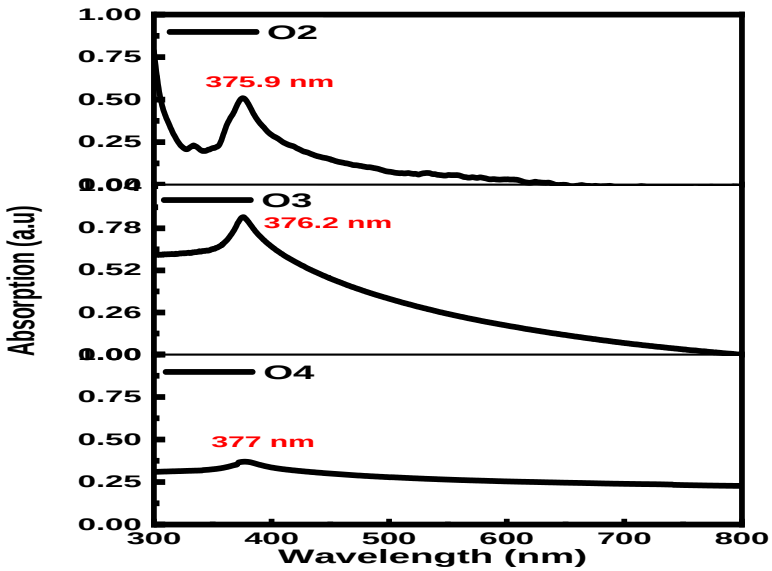

Figure 4. UV-VIS spectra of ZnO NPs synthesized at different CT.

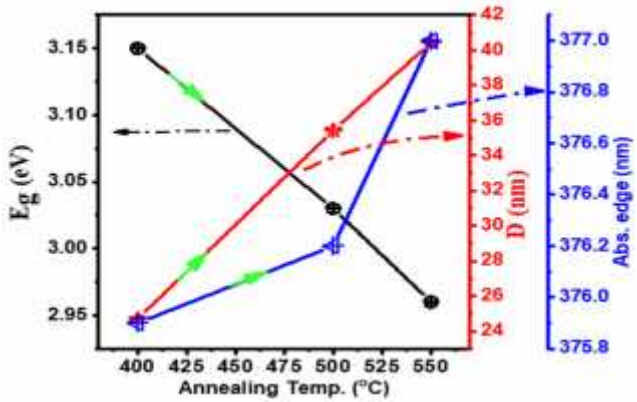

Figure 5. Variation of the energy gap of ZnO NPs synthesized

4.4. Absorption Of Dyes

Figure 6 display the UV-VIS absorption spectra of three of Xanthan dyes (EY, EB and RB) dissolved in absolute ethanol separately. Figure 6, shows that the maximum absorption peak of EY, EB and RB at 526 nm, 534 nm, and 543.5 nm, respectively and also the EB has one small peak around 408.2 nm. EY exhibits a powerful absorption peak in the visible region and its spectrum covers broader window compare to the others. The difference in the absorption characteristics is due to the different of colors of the dyes. The observed absorption peaks in the spectral range between 449 nm and 582 nm represent a part of energy losses in the transition in the UV region. In the DSSCs application, it is much of interests to concentrate in the visible solar spectrum. In addition, to that the molar extinction coefficient of EY equals 112,000 $(cmM)^{-1}$ [21] which is greater than that of RB (106,000 $(cmM)^{-1}$) [22] and much higher than that of EB (50620 $(cmM)^{-1}$) [23], corresponding to $\pi \rightarrow \pi^*$ transitions of conjugated molecules. This may explain the higher performance of DSSCs using EY above that using of other dyes.

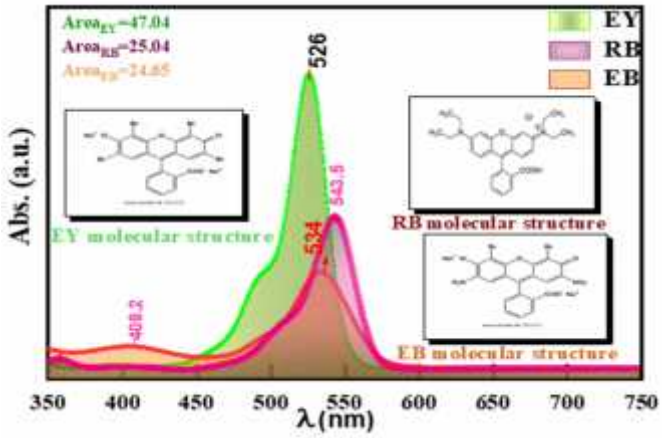

Figure 6. The absorption spectrum of the used dyes dissolved in pure ethanol

4.5. Photoluminescence Spectroscopy

Figure 7 illustrates the PL spectra of the synthesized ZnO. A multiple peak Gaussian curves fit was used to fit the PL spectra of the samples O1, O2, and O3, which reveals that there are four main emission peaks (I, II, III, and IV). Peak (I) positioned at 388.5 nm, is emission near band edge in the UV region. Peak (II) positioned at 412.4 nm, purple color was associated with the recombination of electrons in the Valance band (V.B) to the holes in Zn vacancy band (V_{Zn}), which acts as an acceptor energy level [14]. Peak (III) appears clearly at 451.3 nm (blue emission band) is due to recombination between electrons in the Zn interstitial states (I_{Zn}), which acts as donor energy levels to the holes in the V_{Zn}. Peak (IV) positioned at 650 nm, which reveals a red emission of ZnO NPs. Red emission is attributed to recombination of electrons transition from the I_{Zn} to the oxygen interstitial state (O_i)[24]. Remarkable shift of the maximum peaks towards the higher wavelength with increasing CT. This indicates that there is an increasing in the particle size[16].

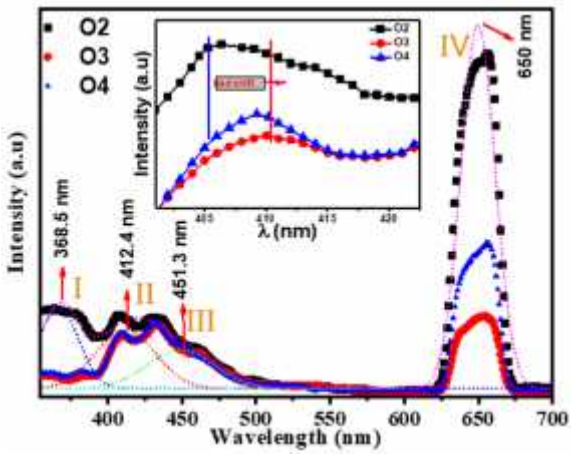

Figure 7. PL spectra of ZnO NPs at different CT.

4.6. Photoelectrchemical Parameters

The performance of the fabricated DSSCs sensitized with Eosin B (EB), Eosin Y (EY) and Rhodamine B (RB) was evaluated by calculating the following Photoelectrchemical parameters: open circuit voltage (V_{oc}), short circuit current density (J_{sc}), the maximum power (P_m), maximum voltage (V_m), maximum current density (J_m), Fill Factor (FF) and efficiency (η). O2 ZnO NPs sample that was used as a selected semiconductor layers for the DSSCs, O2 ZnO NPs sample was examined with three low price sensitizer dyes EB, EY and RB. The characteristics curves, J-V curves and P-V curves are depicted in Figure 8 and Figure 9. The obtained data are listed in Table II. The best efficiency was obtained for EY which has the following results, V_{oc} = 0.52 V, J_{sc} = 4.25 mAcm^{-2}, P_m = 1.08 mWcm^{-2}, FF = 50.08 %, and η = 1.08 %. Using EY as a photosensitizer improved the efficiency. The previous results showed an enhancement of the J_{sc} and the V_{oc} of the EY rather than that of the EB and RB, which may be attributed to broader range of absorption with respect to the others, and it, has higher intensity as depicted in Figure 6. Also, EY has the higher dye loading of the EY on the surface of the ZnO NPs as depicted in previous work [25]. This leads to harvest high amount of photo energy of the sun light.

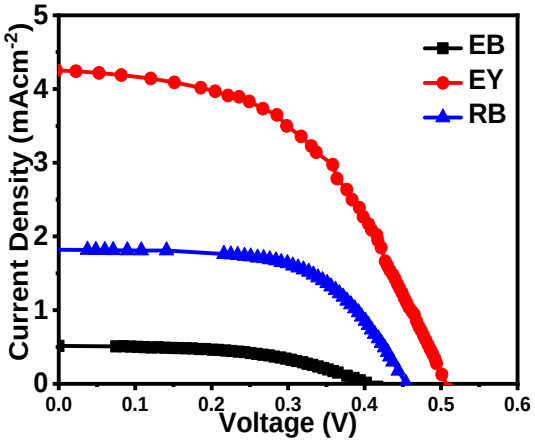

Figure 8 J-V characteristic curves of the DSSCs O2 of ZnO NPs, using EB, EY and RB dyes.

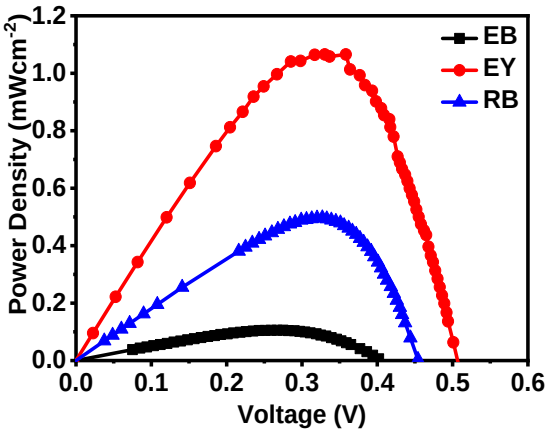

Figure 9 P-V characteristic curves of the DSSCs O2 of pure ZnO NPs, using three dyes.

Table 2. Photoelectrochemical parameters of the DSSCs of ZnO NPs based on (O2, O3 and O4) ZnO NPs using EB as a photosensitizer

Dye	J_{sc} ($mAcm^{-2}$)	V_{oc} (V)	J_m ($mAcm^{-2}$)	V_m (V)	P_m ($mAcm^{-2}$)	FF %	η %
EB	0.52	0.41	0.39	0.28	0.11	50.62	0.11
EY	4.25	0.52	3.19	0.34	1.08	50.08	1.08
RB	2.62	0.51	1.94	0.37	0.72	53.80	0.72

5. Conclusion

In this study, highly purity wurtzite hexagonal phase of ZnO NPs were synthesized by sol-gel technique at different calcination temperature. The calculated average particle size, from XRD increased from 24.7 to 40.4 nm with increasing calcination temperature. UV-VIS results reveled that ZnO NPs has strong absorption spectra in UV region. ZnO NPs have exhibited a direct optical bandgap can be tuned from 3.15 eV to 2.96 eV and its photoluminescence spectra exhibited a violet-blue emission peak at about 405 nm with small red shift, where the temperature increases from 400 oC to 550 oC. Eosin Y exhibited higher efficiency than other xanthene dyes. The best performance was obtained for the DSSC based on O2 ZnO NPs sample sensitized with Eosin Y with photoelectrochemical parameters of VOC = 0.52 V, JSC = 4.25 $mAcm^{-2}$, FF = 50.08 % and η = 1.08%.

6. Acknowledgment

This research activity carried out between Gaza-Palestine and Cairo-Egypt, which was financially supported by Qatar Charity IBHATH Project grant funded by the Gulf Cooperation Council for the Reconstruction of Gaza through the Islamic Development Bank.

7. References

[1] L. He, Z. Tong, Z. Wang, M. Chen, N. Huang, and W. Zhang, "Effects of calcination temperature and heating rate on the photocatalytic properties of ZnO prepared by pyrolysis," *Journal of colloid and interface science*, vol. 509, pp. 448-456, 2018.

[2] Y. Wu, Z.-C. Zhang, and S. Ahmed, "First-Principles Investigation of Size-Dependent Piezoelectric Properties of Bare ZnO and ZnO/MgO Core-Shell Nanowires," *Superlattices and Microstructures*, 2018.

[3] M. Saadeldin, O. A. Desouky, M. Ibrahim, G. Khalil, and M. Helali, "Investigation of structural and electrical properties of ZnO varistor samples doped with different additives," *NRIAG Journal of Astronomy and Geophysics*, 2018.

[4] H. M. H. Zayed, S. Shaat, A. Issa, N. Shurrab, J. Asaad, N. AlDahoudi, "Synthesis of Zinc Oxide nanoparticles at different aging time for low cost Dye Sensitized Solar Cells," *Journal of Scientific Research for Science*, vol. 24, 2017.

[5] J. Luo, J. Lin, N. Zhang, X. Guo, L. Zhang, Y. Hu, Y. Lv, Y. Zhu, and X. Liu, "Eu and F co-doped ZnO-based transparent electrodes for organic and quantum dot light-emitting diodes," *Journal of Materials Chemistry C*, vol. 6, no. 20, pp. 5542-5551, 2018.

[6] S. Shaat, H. Zayed, H. Musleh, N. Shurrab, A. Issa, J. Asad, and N. Al Dahoudi, "Inexpensive organic dyes-sensitized zinc oxide nanoparticles photoanode for solar cells devices," *Journal of Photonics for Energy*, vol. 7, no. 2, pp. 025504-025504, 2017.

[7] M. I. Khalil, M. M. Al-Qunaibit, A. M. Al-Zahem, and J. P. Labis, "Synthesis and characterization of ZnO nanoparticles by thermal decomposition of a curcumin zinc complex," *Arabian Journal of Chemistry*, vol. 7, no. 6, pp. 1178-1184, 2014.

[8] H. Agarwal, S. V. Kumar, and S. Rajeshkumar, "A review on green synthesis of zinc oxide nanoparticles–An eco-friendly approach," *Resource-Efficient Technologies*, 2017.
[9] A. K. Zak, W. A. Majid, M. E. Abrishami, and R. Yousefi, "X-ray analysis of ZnO nanoparticles by Williamson–Hall and size–strain plot methods," *Solid State Sciences*, vol. 13, no. 1, pp. 251-256, 2011.
[10] N. Kaneva, and C. Dushkin, "Preparation of nanocrystalline thin films of ZnO by sol-gel dip coating," *Bulg Chem Commun*, vol. 43, pp. 259-263, 2011.
[11] S. A. S. Naji M. AlDahoudi, Nabil K. Shurrab, Ahmed A. Issa, Hussam S. Musleh, Jehad A. Asaad, Hamdia A. Zayed, "Influence of Metal Ion Doping of Zinc Oxide Photoanode on the Efficiency of Dye Sensitized Solar Cell," *IUG Journal of Natural Studies*, no. Special Issue, March, 2017, pp. 155-159, 14-03-2017, 2017.
[12] A. B. Khatibani, and M. Abbasi, "Effect of Fe and Co doping on ethanol sensing property of powder-based ZnO nanostructures prepared by sol–gel method," *Journal of Sol-Gel Science and Technology*, vol. 86, no. 2, pp. 255-265, 2018.
[13] T. P. B. Karthikeyan, K. Mangaiyarkarasi, "Optical properties of sol–gel synthesized calcium doped ZnO nanostructures," *Spectrochimica Acta Part A: Molecular and Biomolecular Spectroscopy*, vol. 82, pp. 97– 101, 2011.
[14] V. Kumar, H. C. Swart, O. M. Ntwaeaborwa, R. E. Kroon, J. J. Terblans, S. K. K. Shaat, A. Yousif, and M. M. Duvenhage, "Origin of the red emission in zinc oxide nanophosphors," *Materials Letters*, vol. 101, pp. 57-60, 2013/06/15/, 2013.
[15] P. Bindu, and S. Thomas, "Estimation of lattice strain in ZnO nanoparticles: X-ray peak profile analysis," *Journal of Theoretical and Applied Physics*, vol. 8, no. 4, pp. 123-134, 2014.
[16] T. M. Hammad, J. K. Salem, and R. G. Harrison, "The influence of annealing temperature on the structure, morphologies and optical properties of ZnO nanoparticles," *Superlattices and Microstructures*, vol. 47, no. 2, pp. 335-340, 2010.
[17] K. C. S. Hiten Sarma, "X-ray Peak Broadening Analysis of ZnO Nanoparticles Derived by Precipitation method" *International Journal of Scientific and Research Publications*,vol. 4, no. 3, pp. 1-7, March 2014, 2014.
[18] P. Kumbhakar, D. Singh, C. Tiwary, and A. Mitra, "Chemical synthesis and visible photoluminescence emission from monodispersed ZnO nanoparticles," *Chalcogenide letters*, vol. 5, no. 12, pp. 387-394, 2008.
[19] R. R. Harish Kumar, "Structural and Optical Characterization of ZnO Nanoparticles Synthesized by Microemulsion Route," *International Letters of Chemistry, Physics and Astronomy*, vol. 14, pp. 26-36, 2013.
[20] J. K. S. Talaat M. Hammad, Roger G. Harrison "The influence of annealing temperature on the structure,morphologies and optical properties of ZnO nanoparticles," *Superlattices and Microstructures*, vol. 47, pp. 335-340, 2010.
[21] J. M. Dixon, M. Taniguchi, and J. S. Lindsey, "PhotochemCAD 2: a refined program with accompanying spectral databases for photochemical calculations," *Photochemistry and photobiology*, vol. 81, no. 1, pp. 212-213, 2005.
[22] F. S. h. o. o. s. P. d.-a. Eastman Laboratory Chemicals Catalog No. 55 (1993-94).
[23] N. Math, L. Naik, H. Suresh, and S. Inamdar, "Dual fluorescence and laser emissions from fluorescein-Na and eosin-B," *Journal of luminescence*, vol. 121, no. 2, pp. 475-487, 2006.
[24] R. M. Mehmood S, Ismail H, Mirza B, Bhatti AS "Significance of postgrowth processing of ZnO nanostructures on antibacterial activity against gram-positive and gram-negative bacteria," *International journal of nanomedicine* vol. 10, no. 1, pp. 4521-4533, 2015.
[25] N. A. H. Musleh, H. Zayed, S. Shaat, H. M. Tamous, N. Shurrab, A. Issa, J. Asad, A. Al-Kahlout "Synthesis and characterization of ZnO nanoparticles using hydrothermal and sol-gel techniques for dye-sensitized solar cells," *Journal of University of Babylon, Engineering Sciences*, vol. 27, no. 2, 2018.